# An experimentally informed 1-D DDT model for smooth narrow channels

J. Melguizo-Gavilanes[1], L. Bauwens[2]
[1]Institut Pprime, UPR 3346 CNRS, ISAE–ENSMA
86961 Futuroscope-Chasseneuil, France
[2]Department of Mechanical and Manufacturing Engineering
University of Calgary, T2N 1N4 Calgary, AB, Canada

## 1 Introduction

The flame position as a function of time, $x_f$ vs. $t$, can be very accurately determined in optically accessible channels or tubes equipped with photodiodes [1, 2]. These $x_f - t$ diagrams arguably contain the combined effect of momentum and energy losses during flame acceleration (FA) and detonation onset (DO) known to play a role in narrow channels. However, measuring the spatial and temporal variations in pressure, temperature and species concentrations in the gas is not trivial. Likewise, properly simulating the early combustion processes remain very challenging to say the least. Thus, rather than attempting to simulate the whole entire evolution through direct numerical simulations (DNS), where all the fundamental processes are inevitably obscured, our approach seeks to isolate, to the extent possible, the main physics driving the phenomenon by exploiting synergies between experiments and low-order models.

Here, we present our first attempt at developing such models in which experimental $x_f - t$ diagrams are used together with the 1-D reactive Euler equations to investigate the gas dynamics ahead of an accelerating flame in a simple way. Note that the main limitation of the proposed approach is that the flame is assumed to be an infinitely thin reactive discontinuity separating fresh and burnt gases, hence there is no possible flame structure-reactive gas feedback, which was recently suggested as a possible mechanism responsible for FA and transition to detonation [3]. However, the positive feedback between the high speed propagation of the flame brush and the flame generated compressive heating of the unburned medium, as well as the acoustics behind/ahead of the front, are retained.

The main objective of this contribution is thus to investigate the chemical and gas dynamics aspects of FA and DO through experimentally informed simulations.

## 2 Physical model

Rather than attempting to reduce the effects of combustion to an equivalent one-dimensional flame front velocity, the actual front location from experiments is read and an equivalent speed or burning velocity, $s_{\text{eq}}$,

Correspondence to: josue.melguizo-gavilanes@cnrs.prime.fr 

is then derived using $u_f = dx_f/dt = u(p_+, T_+) + s_{\text{eq}}$ where $u(p_+, T_+)$ is the flow velocity immediately ahead of the front.

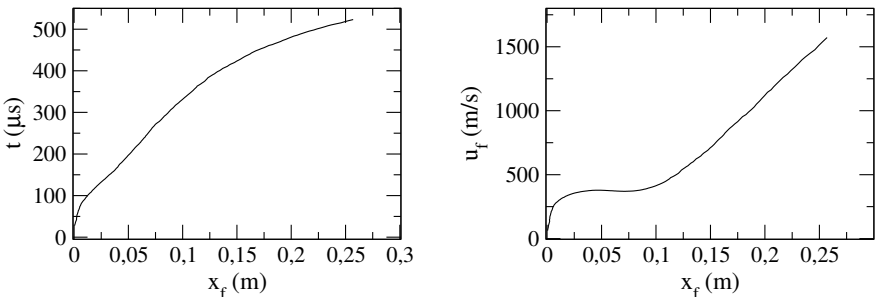


Figure 1: Left: experimentally obtained flame front position time history, $x_f$ for a stoichiometric $H_2$-$O_2$ mixture at $p_0 = 100$ kPa and $T_0 = 300$ K propagating in a 1-m long channel of square cross-section ($6\,\text{mm} \times 6\,\text{mm}$); only the flame acceleration phase is shown. Right: computed flame front velocity, $u_f$, as a function of flame front position.

Initially, $s_{\text{eq}}$ is small compared to the speed of sound, as in [4]. However, as expected and shown in the experimental data, as the front accelerates, its speed can no longer be taken as small compared with the speed of sound (see Figure 1). In [4] and in the early stages here, given that the time step in the simulation is limited by the CFL condition based upon the front speed, $u_f$, the front stays within a given computational cell for many time steps, and proper resolution of the processes requires a subgrid model tracking its location within the computation cell. However later on when the front speed is no longer small, proper front tracking needs to be based upon the full Rankine-Hugoniot equations (RH). Thus, while the code, as in [4], implements a one-dimensional compressible Euler solver for the tube length as a whole, a subgrid model satisfying the full RH condition is required, which then can no longer be dealt with in closed form and requires an iterative solution at each time step.

Consistent with the second order accuracy of the gas dynamics solver, profiles within the cell, on both sides of the front, are taken as linear. Two dummy cells are introduced, allowing for the solver to deal transparently with the front region, determining the solution at the next time step in the two grid points left and right of the front. Then the dummy cells are populated based upon the front model, with values at the precise front location extrapolated linearly.

Between interpolation, for pressure, density and velocity, and the three RH relations, six equations are obtained, which fully determine the jumps at the front location, but, as mentioned above, require an iterative solution. This is done at both predictor and corrector stages. Finally, the front position is updated based upon the experimental data, and the corresponding equivalent one-dimensional burning velocity is calculated.

As to the gas dynamics in the tube, the simulation is effectively as in [4], to which a reactive heat source was added in the unburned region ahead of the front. Namely, it relies upon a second order accurate ENO solver that has been extensively used over the years and is well validated [5–7].

## 3 Results and discussion

Results were obtained using the experimental front position data presented in [3] and shown here for completeness (see Figure 1 - left), with a single-step Arrhenius model in which the rate of fuel consumption

is given by $\dot{\omega}_{\rm F} = \rho(1 - Y_{\rm P})A_s \exp(-\tilde{E}_a/R_u T)$, symbols $\rho$, $A_s$, $Y$, and $\tilde{E}_a/R_u$ denote the gas density, pre-exponential, mass fraction, and reduced activation temperature; subscripts $F$ and $P$ refer to the fuel and product, respectively. The reactive mixture is defined by its ratio of specific heats, $\gamma = 1.4$, and a total heat release of $Q = 20.744$ scaled by the enthalpy in unburned mixture (i.e., a density ratio of $\sim 7$ across the flame front), representative of a stoichiometric $H_2$-$O_2$, mixture for which the experimental data was collected. A numerical domain of 1-m in length was used and discretized in $25 \times 10^3$ points (i.e, $\Delta x = 4\,\mu$m).

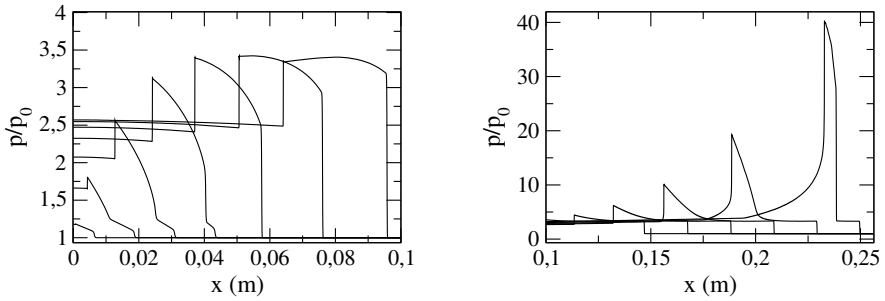


Figure 2: Normalized pressure profiles, $p/p_0$, as the flame front accelerates. Left: initial stages ($0 \leq x\,(\mathrm{m}) \leq 0.1$). Right: late stages ($0.1 \leq x\,(\mathrm{m}) \leq 0.25$). Time interval between consecutive lines is $36\,\mu$s.

Of significance, the velocity reached by the flame front before detonation onset occurs experimentally is quite high or the order of 1500 m/s (see Figure 1 - right). As a result, the pressure ahead of the front should also be high. Furthermore, because the front velocity, after initially increasing, eventually stabilizes and even drops slightly before increasing even faster, leading pressure coalesces into two waves. This can be seen in Figure 2 (left) where normalized pressure profiles are shown for the first 10 cm of the channel for a reduced activation energy, $E = \tilde{E}_a/R_u T_0 = 47$ and $A_s = 6.94 \times 10^9\,\mathrm{s}^{-1}$. The initially weak pressure waves steepen up into a shock with a pressure ratio of about 3; the distance between the flame front and shock is of about 3 cm.

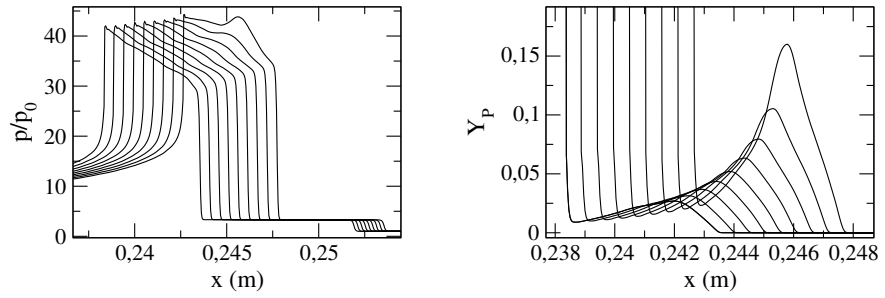


Figure 3: Early stages of hot spot formation. Left: normalized pressure profiles, $p/p_0$. Right: product mass fraction profiles, $Y_{\rm P}$ (right) for a reduced activation energy of $E = 47$. Time interval between consecutive lines is $0.36\,\mu$s.

As the flame front leaves the plateau ($x_f > 0.1$ m) and accelerates abruptly (i.e., $\Delta u_f \sim 1175$ m/s in $150\,\mu$s), it compresses the mixture that had already been shocked and a new, significantly stronger shock with a pressure ratio of $\sim 10$ forms about 5 mm ahead of the front; (see last profile in Figure 2 - right). Note

that the pressure maximum in the channel increases by an order of magnitude during the second acceleration phase, and there is an approximately linear increase in pressure between the newly formed secondary shock and the flame front (location where the maximum is located) . It is precisely in this region where a hot spot forms. Its evolution over $3.6\,\mu$s is shown in Figure 3; the incipient localized pressure increase is accompanied by an initially distributed fuel consumption that quickly narrows into the peak visible in the product mass fraction plot.

Figure 4 (left) is closeup view of the region between the flame front and secondary precursor shock wave, which initially contains partially reacted mixture. Earlier evolution shows that the flame acceleration is so strong that it quickly brings the gas to thermodynamic conditions that are favorable for a hot spot to form and grow rapidly. This explosion center evolves into two self-sustained waves: one moving left towards the flame front, and the other one moving right towards the secondary precursor shock wave. Figure 4 (right) shows them steepening up into detonation waves propagating in that zone already pre-heated by the precursor shock wave. The left-moving wave eventually reaches the original reaction front, whereas the right moving one reaches the precursor shock and continues as a weaker wave upon their interaction.

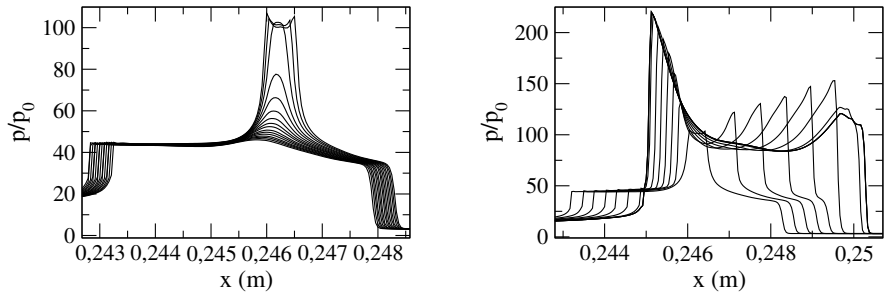


Figure 4: Normalized pressure profiles, $p/p_0$, for a reduced activation energy of $E = 47$. Left: hot spot formation. Right: detonation onset. Time intervals between consecutive lines are $0.018\,\mu$s (left) and $0.18\,\mu$s (right).

Note that classical work [8] describing deflagration-to-detonation transition (DDT) in narrow channels, using a 1-D Navier-Stokes formulation with friction losses, results in DDT but in a qualitatively different way. The authors describe an extended preheat zone in which a reaction front emerges, however, here we show the crucial role played by the late flame acceleration stage in forming a stronger precursor shock that is then responsible for detonation onset. Recent work by Clavin and Tofaili [9], inspired by a largely overlooked paper by Deshaies and Joulin [10], alludes to the role of compressibility and the possibility of shock formation near flame fronts as a potential DDT mechanism for mixtures with large expansion ratios. The integration of the experimental data with a gas dynamics solver, as done in this work, allows to elucidate this as well as the subsequent stages of the DDT evolution.

Next, results were obtained, based upon the same flame front time history, for a reduced activation energy more representative of stoichiometric $H_2$-$O_2$ at ambient conditions, i.e., $E = 30$. Note that the pre-exponential factor was modified to $A_s = 11.22 \times 10^9$ s$^{-1}$. The results are shown in Figure 5 (top) and closely resemble those obtained for $E = 47$ except that the initial hot spot is not as narrow, and the pressure peak attained at the flame front is slightly lower. The combination of a higher $A_s$ together with a lower $E$ results in a higher reaction rate so that a hot spot appear sooner. These results are somewhat expected based on previous shock-induced ignition studies such as [11].

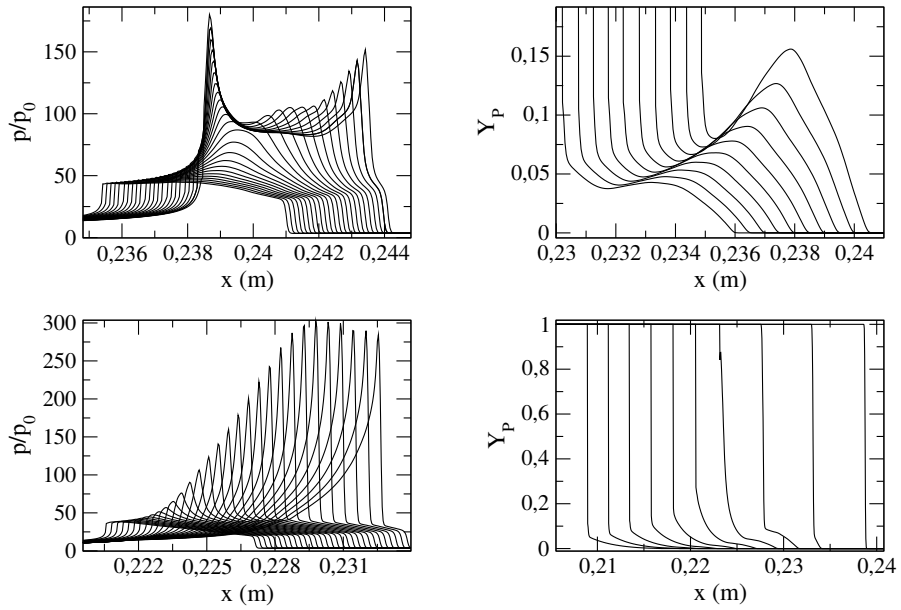


Figure 5: Effect of reduced activation energy, $E$, on hot spot formation and detonation onset. Normalized pressure, $p/p_0$, and product mass fraction profiles, $Y_P$. Top row: $E = 30$; time intervals between consecutive lines are $0.09\,\mu$s for $p/p_0$ and $0.18\,\mu$s for $Y_P$. Bottom row: $E = 28$; time intervals between consecutive lines are $0.36\,\mu$s for $p/p_0$ and $3.6\,\mu$s for $Y_P$.

A further decrease in reduced activation energy to $E = 28$ hence even higher reactivity leads to different results (see Figure 5 bottom). There is no longer a clear hot spot forming; a wider interval is now reacting, with spatial extent starting close to the flame front. As a result, only a right-going detonation front appears which will eventually reach the precursor shock wave. While the peak pressure is higher, it is no longer located at the flame front and starts dropping even before reaching the precursor wave. The stark change in behavior for such a small decrement in $E$ may suggest that the modeled mixture no longer mimics the experimental flame front data. Because at lower $E$ the reaction is stronger and occurs earlier, while the leading pressure wave is still steepening (see Fig. 2), temperature in this interval peaks at the flame front. In contrast, for the less reactive cases (i.e., higher $E$) reaction occurs later, when temperature peaks closer to the leading shock, hence the different behavior with a noticeable hot spot appearing. Finally, for $E = 30$ and 28, transition occurs before it does in the experiments, which may indicate that reactivity is too high in the simulations; the results for $E = 47$ might thus be closer to reality.

## 4 Conclusion

A gas dynamical model was introduced in which synergies between experiments and low-order numerical simulations are exploited. Notably the role of the late stages of flame acceleration in forming a significantly stronger secondary precursor shock very close to the flame front was elucidated. Future work will include: (i) testing the current model with experimental $x-t$ diagrams for varying $N_2$ dilution levels until DDT is not observed in the available channel length (i.e., $H_2$-Air); (ii) studying the effect of more complex simplified kinetic schemes (i.e. three/four-step chain-branching); (iii) generalizing the front model to detailed kinetics

with the objective of determining critical FA rates for fuels of practical interest.

## Acknowledgements

Financial support from the Agence Nationale de la Recherche Program JCJC FASTD ANR-20-CE05-0011-01 (JMG) and the Natural Sciences and Engineering Research Council of Canada (LB) is gratefully acknowledged.

## References

[1] H.-W. Ssu and M.-H. Wu, "Formation and characteristics of composite reaction–shock clusters in narrow channels," *Proceedings of the Combustion Institute*, vol. 38, no. 3, pp. 3473–3480, 2021.

[2] M. Kuznetsov, V. Alekseev, I. Matsukov, and S. Dorofeev, "DDT in a smooth tube filled with a hydrogen–oxygen mixture," *Shock waves*, vol. 14, no. 3, pp. 205–215, 2005.

[3] J. Melguizo-Gavilanes, Y. Ballossier, and L. Faria, "Experimental and theoretical observations on DDT in smooth narrow channels," *Proceedings of the Combustion Institute*, vol. 38, 2020.

[4] L. Bauwens, C. R. L. Bauwens, and I. Wierzba, "Oscillating flames: multiple-scale analysis," *Proceedings of the Royal Society A: Mathematical, Physical and Engineering Sciences*, vol. 465, no. 2107, pp. 2089–2110, 2009.

[5] Z. Liang and L. Bauwens, "Detonation structure with pressure-dependent chain-branching kinetics," *Proceedings of the Combustion Institute*, vol. 30, no. 2, pp. 1879–1887, 2005.

[6] L. Bédard-Tremblay, L. Fang, J. Melguizo-Gavilanes, L. Bauwens, P. Finstad, Z. Cheng, and A. Tchouvelev, "Simulation of detonation after an accidental hydrogen release in enclosed environments," *International journal of hydrogen energy*, vol. 34, no. 14, pp. 5894–5901, 2009.

[7] J. Melguizo-Gavilanes and L. Bauwens, "A comparison between constant volume induction times and results from spatially resolved simulation of ignition behind reflected shocks: implications for shock tube experiments," *Shock Waves*, vol. 23, no. 3, pp. 221–231, 2013.

[8] I. Brailovsky and G. I. Sivashinsky, "Hydraulic resistance as a mechanism for deflagration-to-detonation transition," *Combustion and flame*, vol. 122, no. 4, pp. 492–499, 2000.

[9] P. Clavin and H. Tofaili, "A one-dimensional model for deflagration to detonation transition on the tip of elongated flames in tubes." *Combustion and Flame*, vol. 232, p. 111522, 2021.

[10] B. Deshaies and G. Joulin, "Flame-speed sensitivity to temperature changes and the deflagration-to-detonation transition," *Combustion and flame*, vol. 77, no. 2, pp. 201–212, 1989.

[11] J. Melguizo-Gavilanes, N. Rezaeyan, M. Lopez-Aoyagi, and L. Bauwens, "Simulation of shock-initiated ignition," *Shock Waves*, vol. 20, no. 6, pp. 467–478, 2010.